GERARD Q CRATER REGION, MOON: KREEP INDUCED VOLCANISM IN MARE-HIGHLANDS BOUNDARY? Hephzibah Christopher[1], N.Kumari[2], K. Shanmugapriya[1,] S.Vijayan[3] [1]Institute of Remote Sensing, College of Engineering, Chennai, India. [2]Department of Geosciences, Stony Brook University, Stony Brook, NY, USA. [3]Planetary Science Division, Physical Research Laboratory, India. hephzy25@gmail.com, Nandita.kumari@stonybrook.edu, vijayan@prl.res.in

Introduction: Impact craters located on the mare-highland boundaries with volcanic deposits on their floor have raised concerns regarding the lateral/vertical magma distribution in the crust, infilling, mineralogy, and chronology. The significant topographic and crustal variations in the mare-highland boundary demand a detailed study about how the craters and the infilling within them is affected. While the influence of a subsurface KREEP layer in mare volcanism had been evidenced in the western nearside basalts [1], there is little understanding about its relation to the other last stage mare eruptions. We report a potential Procellarum KREEP Terrane (PKT) volcanic activity in Gerard Q Inner (GQI) crater located on the western margin of Oceanus Procellarum. Gerard Q Inner is a ~67 km diameter crater situated within another impact crater, Gerard Q Outer (GQO), whose diameter is ~192 km (Fig.1a). The formation/location of Gerard Q complex on the transition boundary between mare and highlands makes it a compelling site to be studied in detail to unravel the lunar volcanic history.

Datasets and methods: We have used LROC Wide Angle Camera (WAC) global mosaic of ~100m/px for morphological analysis. Kaguya-Selene DEM (~7m/px) has been used for topographical analysis (Fig.1b). The mineralogical analysis has been performed using Chandrayaan-1 Moon Mineralogy Mapper (M^3) dataset of ~240m/px resolution from OP2C2 optical period. A second-degree smoothening of M^3 data is used to reduce the spikes. The tie points for the continuum removal have been set ~700 nm and ~2576 nm. The band centers have been calculated from a python routine using spline fit over the bands near 1000/2000 nm. Integrated Band Depths (IBD) have been derived for 1 and 2 µm bands to delineate the mafic compositions. For chronology, craters >300 m are counted from Narrow-Angle Camera (NAC) images of ~2 m/px. Crater size-frequency distributions were computed using Craterstats [2].

Results and Discussion: Topography: Selene topography data shows that GQO has a convex-up floor profile (Fig.1d). The topography of GQI is irregular, with many uplifted blocks within the crater. Furthermore, there are multiple fractures of varying dimensions dissecting the crater floor. The elevation along the GQI rim is varying, while the inner knob is elevated more than the crater rim. Fig.1d also reveals that the central knob is almost elevated higher than the crater rim.

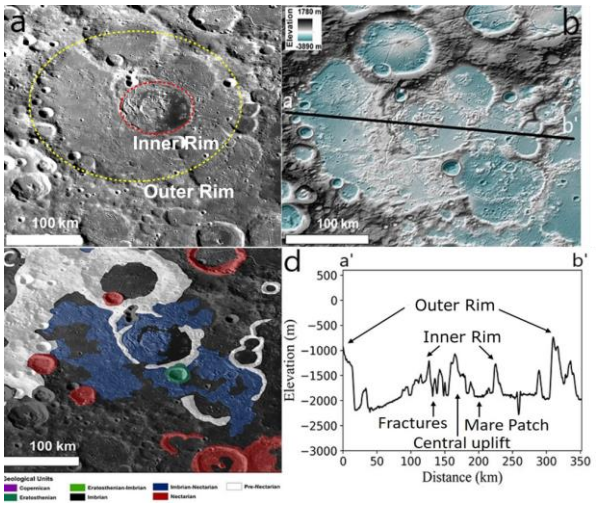

Fig 1. *a) LROC WAC mosaic of Gerard Q Inner crater superposed on Gerard Q Outer. b) SELENE topographic map. c) Unified geologic map of the study area as provided by [3]. d) Elevation profile along the transect in 1b. GQO shows an up-bowed topography to the west of GQI rim.*

Geomorphology: Gerard Q Inner belongs to class 3 floor-fractured craters as defined by [4]. GQI accommodates irregular uplift platforms of varying sizes, thus giving the floor a hummocky appearance. The knobs are separated by numerous narrow as well as wide fractures. The central knob is broad, intersected by fractures in W-NE, N-SE trends. It hosts a shallow central peak. Small, isolated knobs are seen in the mare inundated eastern and northern crater floor. More flat-topped blocks are concentrated on the south-western and western sides of GQI. The fractures observed in GQI exhibit varied morphology. A large fracture extends from crater Galvani, located NE to GQI, whereas another graben cuts through the SE rim The northern rim is not well defined and is discontinuous. About ~30% of the crater floor area is flooded by mare basalts. There are two major crescent-shaped magma units on either side of the central knob. There is a smaller mare unit south-west to the central knob. The volcanic units are compartmentalized with respect to differences (~60 m) in elevation. GQO has uplifted floor and no evidence for visible mare patches.

Mineralogy: In Fig.2a, the yellow pixels indicate strong mafic absorption in both 1 and 2 µm bands. Blue regions are highland materials lacking Fe^{2+} absorption. In Fig. 2b the BC1 Vs BC2 plot shows pyroxene distribution in the Gerard Q region.

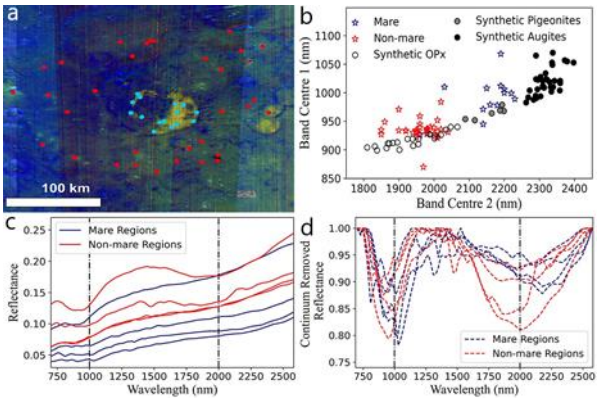

Fig 2. *a)M³ IBD composite (R=IBD at 1 μm, G=IBD at 2 μm and B = M³ reflectance at 1.58 μm). Red and blue dots are mare and non-mare locations respectively, where spectra are collected. b) BC1 Vs BC2 plot for the spectra compared with synthetic pyroxenes collected by [5,6] c) M³ reflectance spectra collected in 2a d) their corresponding continuum removed reflectance.*

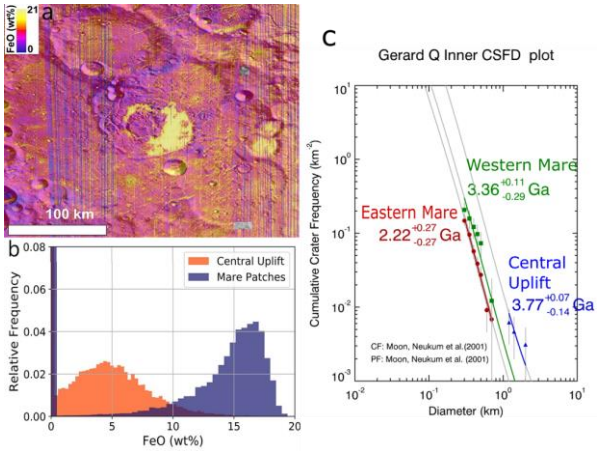

Fig 3. *a) FeO abundance map for Gerard Q region. b) Histogram of FeO wt% of the mare units and central uplift c) CSFD plots for the mare patches and central uplift in GQI.*

Spectra collected from GQO shows low-Ca pyroxene diagnostic absorptions (Fig.2b-d). Of these, the spectra having band centers at short wavelengths have high Mg content, suggestive of noritic lithology of the lower crustal origin or from Mg-suite intrusions. Moderate Mg pyroxene exposures having band centers at slightly longer wavelengths could be mixtures of low Ca-pyroxenes and iron-bearing anorthosites. Clinopyroxenes are detected in the GQI basalts. We used M³ 750 nm and 950 nm reflectance values to map FeO abundance in the Gerard Q region by following [7]. Fig.3a-b shows that mare deposits within GQI contain high Fe content (wt%>20). Besides that, we noticed high Ti in the mare units as estimated in [8]. The observed high Ti, high Fe content in GQI mare is compositionally similar to the late-stage PKT basalts covering the central parts of Oceanus Procellarum.

Chronology: We constrained absolute model ages for the mare units and the central knob using [9]. To minimize error bars, we excluded secondary crater chains and clusters while counting and corroborated the spectral homogeneity of each of the mare patches using M³ color maps. We found the western mare patch to be emplaced around ~3.36 Ga while the eastern volcanic unit is dated to ~2.22 Ga (Fig.3c). There is a ~1.1 Ga gap between the eruption episodes indicating that volcanism had lasted for longer periods in Gerard Q Inner. Crater counting of central knob yielded an upper age of ~3.78 Ga, suggesting that Gerard Q Inner formed pre-Orientale [10]. The first mare eruption occurred likely on the western side ~420 Ma after the GQI forming event. The eastern mare infilling could have started alongside the western side eruption but lasted until ~2.22 Ga. Alternatively, the eastern unit could have experienced the latest resurfacing at ~2.22 Ga. The prolonged volcanic activity exhibited on the eastern side could be attributed to late-stage PKT volcanism, given its proximity to Oceanus Procellarum. All this infers GQI likely remained as a volcanically active region for more than a billion years.

Summary: Gerard Q Inner is a floor fractured crater that got infilled with extrusive basalts during different periods. While the western mare was emplaced soon after the crater formation, the eastern mare eruption occurred during the last stages of lunar volcanic activity. It is likely caused by magmatic intrusion beneath the crater floor. The presence of many FFC's around GQO and its locality in the mare-highland boundary supports the possible existence of laccolith intrusions [11]. M³ mineralogical analyses reveal that the volcanic deposits are rich in Ti and Fe, thus substantiating the likely occurrence of KREEP related volcanism. Furthermore, LCP, HCP signatures are detected in the Gerard Q region. Detailed geological and compositional mapping of Gerard Q will engender new insights into lunar stratigraphy and thermal evolution at this mare-highland boundary.

References:

[1] Wieczorek M. A. & Phillips R. J. (2000) *JGR*, 105(E8), 20417–20430 [2] Michael G.G. & Neukum G. (2010) *EPSL*, 294(3–4), 223–229. [3] Fortezzo C.M. et al. (2020) *LPSC* 2020 Abstract #2760 [4] Schultz P.H. (1976) *Moon*, 15, 241–273 [5] Klima R.L. et al. *Meteorit. Planet. Sci.*, 42, 235–253 [6] Klima R.L. et al. *Meteorit. Planet. Sci*., 46, 379–395 [7] Zhang W. (2014) *Encyclopedia of Lunar Science. Springer, Cham.* [8] Sato H. et al. (2017) *Icarus*, 296, 216-238 [9] Neukum G. et al, (2001) *Space Science Reviews*, 96(1/4), 55–86 [10] Whitten J. et al. (2011) *JGR*, 116, E00G09 [11] Jozwiak L. M. et al. (2015) Icarus, 248, 424-447